Engineering Fracture Mechanics 223 (2020) 106787

Contents lists available at ScienceDirect

Engineering Fracture Mechanics

journal homepage: www.elsevier.com/locate/engfracmech

A unified mean stress correction model for fatigue thresholds prediction of metals

Yong Liu[a], Marco Paggi[b], Baoming Gong[a,*], Caiyan Deng[a]

[a] Department of Materials Science and Engineering, Tianjin University, Road Weijin 92, Tianjin 300072, China
[b] IMT School for Advanced Studies, Piazza San Francesco 19, Lucca 55100, Italy

ARTICLE INFO

Keywords:
Mean stress effect
Fatigue limit
Stress ratio
Strain energy
Dimensional analysis

ABSTRACT

Two fatigue characteristic thresholds, i.e. fatigue limit $\Delta\sigma_e$ and fatigue crack propagation threshold ΔK_{th}, have significant mean stress sensitivity. In the work, a new mean stress correction model for the two fatigue thresholds is proposed based on the cyclic strain energy density concept. Extensive experimental data in the literature is unified evenly by the proposed normalized fatigue threshold-*R* curves. Besides, a comparison of the proposed model with the existing models is carried out, which demonstrates that the present work can achieve more accurate predictions with the advantage of being of easy use and of being independent on any material constant.

1. Introduction

In fatigue analyses and design, there are two commonly used thresholds: fatigue limit (or endurance limit) $\Delta\sigma_e$ and fatigue crack propagation threshold ΔK_{th}, which correspond to different design philosophies. The fatigue limit is used within the frame of a *safe-life* concept, whereas the fatigue crack propagation threshold is part of a *damage tolerance* design. These two thresholds are usually considered as material properties. However, different from the other material properties such as yield strength and ultimate strength, the fatigue limit and fatigue crack propagation threshold are strongly related to the applied load conditions, rather than intrinsic material constants. It is well known that the mean stress σ_m or stress ratio R of the applied load has a significant effect on $\Delta\sigma_e$ and ΔK_{th} [1,2]. In order to avoid time consuming experimental testing, various mean stress correction methods have been proposed to establish the relationships between the fatigue thresholds and mean stress for different failure modes, materials and environments. Regarding the mean stress effect on fatigue limit $\Delta\sigma_e$, many relations, mostly empirical, were proposed during last decades, such as the well-known Goodman's [3], Gerber's [4], and Smith-Watson-Topper's [5] method, etc. Despite their extensive usage, there exists no consensus on the accuracy and physical basis. Besides, these empirical relationships only give rough estimation of the fatigue limit under different mean stresses, which sometimes deviates seriously from the actual value.

As for the fatigue crack propagation threshold, the models considering the mean stress effect can be classified in two categories. The models in the first category are based on the crack closure theory, where crack closure is considered as a dominant mechanism influencing the fatigue crack propagation behavior including the mean stress effect on fatigue crack propagation threshold. Based on crack closure measurements or analytical crack closure models at different mean stress or stress ratio, an effective ΔK is calculated to unify crack propagation data. The most well-known mean stress equation in this category was proposed by Elber [6]. A complete historic review of the research and development of R-dependence of crack closure has been reported by Zhu et al. [7]. However, the difficulty of this kind of model is the application of crack closure [8]. The second category hosts the equations which are directly

* Corresponding author.
E-mail address: gongbm@tju.edu.cn (B. Gong).

https://doi.org/10.1016/j.engfracmech.2019.106787
Received 8 November 2019; Received in revised form 17 November 2019; Accepted 18 November 2019
Available online 21 November 2019
0013-7944/

Nomenclature

E	Young's modulus
$\Delta\sigma_e$	fatigue limit or endurance limit
ΔK_{th}	fatigue crack propagation threshold
σ_m	mean stress
R	stress ratio
R_{ref}	reference stress ratio
$\Delta\sigma_{eR}$	fatigue limit at stress ratio R
$\Delta\sigma_{e,ref}$	fatigue limit at reference stress ratio
$\Delta\sigma_{e,-1}$	fatigue limit at stress ratio $R = -1$
W_c	critical anelastic dissipative energy
V	stressed material volume
$\frac{W_c}{V}$	critical anelastic dissipative energy density
Δw_e	elastic strain energy density by Kujawski
ΔK_{thR}	fatigue crack propagation thresholds at the stress ratio of R
ΔK_{th0}	fatigue crack propagation thresholds at the stress ratio of 0
$g(R)$	mean stress correction function for ΔK_{th}
α	material-dependent parameter in Kwofie equation
γ	material-dependent parameter in Walker equation
k	material-dependent parameter in Sekercioglu equation
Y	geometric factor
a	crack length

Abbreviations

UTS	ultimate strength stress
TTS	true tensile strength
YS	yield stress
RMSE	root mean squared error

fitted to crack propagation threshold at different mean stresses, such as the well-known Walker's equation [9]. The equations used in the second category usually have the same form as the relation between the fatigue limit and mean stress or stress ratio [10]. From this view, if the mean stress correction model of fatigue limit is well established, it is able to reach a satisfactory mean stress correction model of fatigue crack propagation threshold simultaneously.

In this work, a new mean stress correction model is proposed for fatigue limit prediction of metals based on the assumption that the needed elastic strain energy leading to fatigue failure is identical under different stress ratios. A unified fatigue limit $\Delta\sigma_e$-R correlation can be obtained, and very good correspondence is achieved between the proposed model and experimental data sets in the literature, including steel, aluminum, titanium alloys, magnesium alloys and nickel alloys. Furthermore, a fatigue crack propagation threshold ΔK_{th}-R relationship is established based on the proposed $\Delta\sigma_e$-R correlation and verified by the experimental results. Finally, a comparison of the proposed models with the existing models is carried out and it is found the present models can achieve more accurate predictions with the advantage of being of easy use and of being independent on any material constant.

2. The new mean stress correction model

2.1. R-dependence model of fatigue limit $\Delta\sigma_{eR}$

Fatigue damage evolution is an irreversible thermodynamic process accompanied by energy dissipation [11]. In the high cycle fatigue of metal materials, the dissipative energy can be divided into two parts: anelastic dissipation and inelastic dissipation, neglecting other forms of energy dissipation such as acoustic emission, electricity and magnetism [12]. Anelastic dissipation is caused by internal friction, which involves deformation mechanisms such as reversible movement of dislocations and grain boundaries [13]. According to the damage accumulation theory, the accumulation of microplastic deformation induced by cyclic loading results in fatigue failure, whilst anelastic dissipation does not cause material damage. Inelastic dissipation refers to the energy dissipation due to the formation of the microcracks and microplastic deformation, which is the main factor of fatigue fracture [14]. Fig. 1 illustrates the variation of the dissipative energy vs. the stress range [13]. When the applied stress range is below the fatigue limit, there is no inelastic dissipation since the mechanical behavior of material is mainly related to recoverable microstructure motions. On the

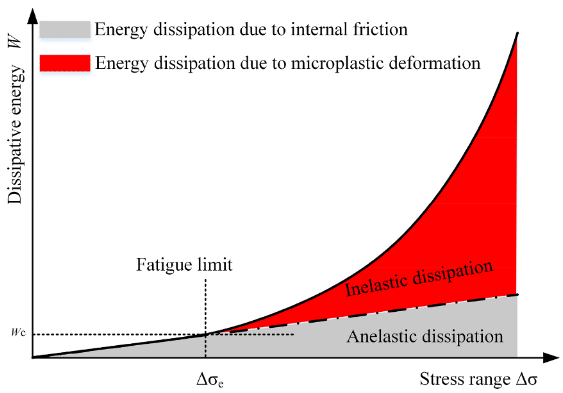

Fig. 1. The schematic diagram of energy dissipation as a function of applied stress range for materials.

contrary, for the applied stress range above the fatigue limit, microplastic deformation appears and induces inelastic dissipation. Accordingly, the fatigue limit of material corresponds to a critical value of anelastic dissipative energy W_c, at which the mechanism of energy dissipation transforms from anelastic dissipation to the combined effect of anelastic dissipation and inelastic dissipation. In the work, the critical anelastic dissipative energy W_c is assumed to be a material constant and used as an indicator to measure the fatigue limit.

The analyzed specimens in the present study are limited to engineering metals and to axially loaded, smooth ones. Naturally, strain energy density can be adopted easily as a characteristic parameter to calibrate the intensity of repeated load for the considered specimens, which is independent of the geometric reference system and represents the parameter necessary for the estimation of fatigue limit of metallic structural components [15]. Accordingly, the critical anelastic dissipative energy W_c can be expressed as the form of strain energy density, $\frac{W_c}{V}$, which can be easily obtained by measuring the area enclosed by stress-strain curve and the coordinate axis as shown in Fig. 2 (V is the stressed material volume). Fig. 2 illustrates a sketch of the strain energy density per cycle at two different stress levels ($R > 0$ and $R < 0$) in the high cycle fatigue regime.

For a stress ratio $R \geq 0$, the strain energy density per cycle can be expressed as:

$$\frac{W_c}{V} = \frac{\sigma_{\max}^2}{2E} - \frac{\sigma_{\min}^2}{2E} = \frac{(1+R)\Delta\sigma^2}{2E(1-R)} \tag{1}$$

while for a stress ratio $R < 0$, the strain energy density per cycle can be expressed as:

$$\frac{W_c}{V} = \frac{\sigma_{\max}^2}{2E} + \frac{\sigma_{\min}^2}{2E} = \frac{(1+R^2)\Delta\sigma^2}{2E(1-R)^2} \tag{2}$$

If the reference fatigue limit $\Delta\sigma_{e,\text{ref}}$ is obtained by experiment at $R_{\text{ref}} \geq 0$, according to the above discussion, the following equation for any $R \geq 0$ can be derived:

$$\frac{(1+R)\Delta\sigma_{eR}^2}{2E(1-R)} = \frac{(1+R_{\text{ref}})\Delta\sigma_{e,\text{ref}}^2}{2E(1-R_{\text{ref}})} \quad (R_{\text{ref}} \geq 0,\ R \geq 0) \tag{3a}$$

If Eq. (3a) is re-formulated, the ratio between the fatigue limit at a stress ratio R and that at the reference mean stress can be obtained as:

$$\frac{\Delta\sigma_{eR}}{\Delta\sigma_{e,\text{ref}}} = \sqrt{\frac{(1+R_{\text{ref}})(1-R)}{(1-R_{\text{ref}})(1+R)}} \quad (R_{\text{ref}} \geq 0,\ R \geq 0) \tag{3b}$$

where $\Delta\sigma_{eR}$ denotes the fatigue limit at stress ratio R.

For $R < 0$, the equation is given as:

$$\frac{(1+R^2)\Delta\sigma_{eR}^2}{2E(1-R)^2} = \frac{(1+R_{\text{ref}})\Delta\sigma_{e,\text{ref}}^2}{2E(1-R_{\text{ref}})} \quad (R_{\text{ref}} \geq 0,\ R < 0) \tag{4a}$$

If Eq. (4a) is re-formulated, the ratio between the fatigue limit at a stress ratio R and that at the reference mean stress can be obtained as:

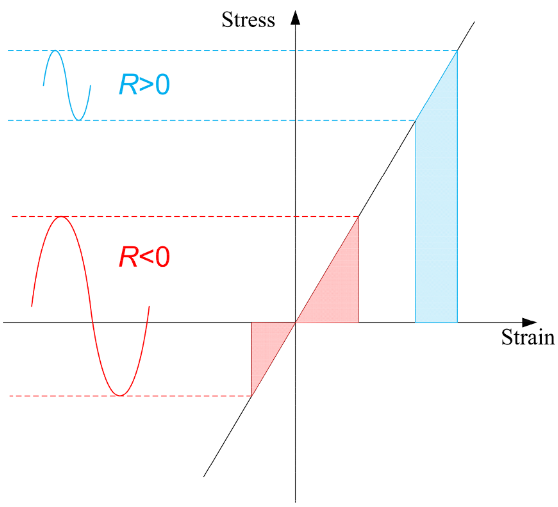

Fig. 2. Schematic diagram of cyclic strain energy density at different stress ratios.

$$\frac{\Delta\sigma_{eR}}{\Delta\sigma_{e,ref}} = \sqrt{\frac{(1+R_{ref})(1-R)^2}{(1-R_{ref})(1+R^2)}} \quad (R_{ref} \geq 0,\ R < 0) \tag{4b}$$

Similarly, if the reference fatigue limit $\Delta\sigma_{e,ref}$ is obtained by experiment at $R_{ref} < 0$, then

$$\frac{\Delta\sigma_{eR}}{\Delta\sigma_{e,ref}} = \sqrt{\frac{(1+R_{ref}^2)(1-R)}{(1-R_{ref})^2(1+R)}} \quad (R_{ref} < 0,\ R \geq 0) \tag{5}$$

$$\frac{\Delta\sigma_{eR}}{\Delta\sigma_{e,ref}} = \sqrt{\frac{(1+R_{ref}^2)(1-R)^2}{(1-R_{ref})^2(1+R^2)}} \quad (R_{ref} < 0,\ R < 0) \tag{6}$$

It should be mentioned here that a previous work by Kujawski et al. [16] also used the elastic strain energy density as an indicator to consider the fatigue limit under different stress ratios. However, in their work, the elastic strain energy density is defined as a constant:

$$\Delta w_e = \frac{\Delta\sigma^2}{2E} \tag{7}$$

Further, a fatigue damage parameter ψ_e, which is assumed to be equal under different stress ratios, is defined as:

$$\psi_e = \Delta w_e f(R) \tag{8}$$

where $f(R)$ is a function of stress ratio. Kujawski et al. [16] used a power law form to define the stress function $f(R)$. In the work, the effect of mean stress or stress ratio is naturally included in the strain energy density as shown in Eqs. (1) and (2), without introducing extra function $f(R)$.

2.2. Modeling R-dependence of fatigue crack propagation threshold ΔK_{thR}

For cracked components, the stress intensity factor range ΔK is usually used to assess the fatigue crack propagation behavior. The fatigue crack propagation threshold ΔK_{th} is the stress intensity factor range below which cracks do not propagate. Since crack growth is due to the tensile portion of the cyclic stress and that compressive loads are less detrimental, the effect of $R > 0$ on crack growth attracts more attention relative to $R = 0$.

$$\frac{\Delta K_{thR}}{\Delta K_{th0}} = g(R) \tag{9}$$

where ΔK_{thR} and ΔK_{th0} are the fatigue crack propagation thresholds at the stress ratio of R and 0, respectively. $g(R)$ is the mean stress correction function for ΔK_{th}. According to the Kitagawa-Takahashi theory [17], the relation between fatigue crack propagation threshold ΔK_{th} and fatigue limit $\Delta\sigma_e$ can be expressed as

$$\Delta K_{th} = Y\Delta\sigma_e\sqrt{\pi a} \tag{10}$$

where Y is the geometric factor and a is the crack length. Accordingly, Eq. (9) can be re-written as

$$\frac{\Delta K_{thR}}{\Delta K_{th0}} = \frac{\Delta\sigma_{eR}}{\Delta\sigma_{e0}} \tag{11}$$

Further, according to Eq. (3b), the mean stress correction model of fatigue crack propagation threshold can be derived as

$$\frac{\Delta K_{thR}}{\Delta K_{th0}} = \sqrt{\frac{1-R}{1+R}} \quad (0 \leq R < 1) \tag{12}$$

It is worth noting that the same equation is also proposed by McEvily [18] to model the R-dependence of ΔK_{th}, but the corresponding reasoning is not provided.

3. Experimental validation

3.1. Validation of the proposed $\Delta\sigma_{eR}$-R model

To verify the accuracy of the proposed $\Delta\sigma_{eR}$-R model, the authors are able to locate a total of 145 experimental data sets at different mean stresses of various materials, including steels, aluminum alloys, titanium alloys, magnesium alloys and nickel alloys. Most of the data sets are summarized in a tabular form in Ref. [19] and some are extracted from the S-N curves using the commercial software GetData when numerical values are not available [20–30]. Besides, special attention should be paid to the experimental data sets of aluminum alloys in Ref. [19], where most of the fatigue limits are determined at a fatigue life of more than 10^8 cycles, indicating that fatigue failure occurs at the stage of the very high cycle fatigue (VHCF). It has been widely studied that there is a significant difference in the failure mechanism between the stages of high cycle fatigue and VHCF [31,32]. In the VHCF regime, the crack usually initiates at the interior of the specimen, which may be dominated by the internal inclusions. Therefore, the present theory cannot be applied to study the fatigue behavior in the VHCF regime. Only the fatigue limits at 10^7 cycles are used in the work.

All data are provided with more details in the Supplement material.

In all the experiments, the fatigue limit $\Delta\sigma_{e,-1}$ at zero mean stress is known, and thus adopted as a benchmark, i.e. R_{ref} is chosen to be -1.0 and $\Delta\sigma_{e,ref}$ is equal to $\Delta\sigma_{e,-1}$. Because of $R_{ref} < 0$, Eqs. (5) and (6) are used to predict the fatigue limit at R range from -1.0 to 1.0. The comparison between the proposed model and the experimental data sets is shown in Fig. 3 with all the fatigue limits normalized by $\Delta\sigma_{e,-1}$ in ordinate axis. In order to assess the universal applicability of the proposed model to engineering metallic materials, Fig. 3a, 3b and 3c compare the proposed model with the experimental data sets of steels, aluminum alloys and other non-ferrous alloys (excluding aluminum alloys), respectively. It can be found that the prediction agrees with experimental results with a satisfactory degree of accuracy. Fig. 3d shows that all data points of each material uniformly collapse into a single normalized fatigue limit $\Delta\sigma_{eR}$-R curve, and the method can describe the mean stress effect on fatigue limits successfully in a unified form.

3.2. Validation of the proposed ΔK_{thR}-R model

R-dependence of fatigue crack propagation threshold, i.e. Eq. (12), is verified by the experimental data from Refs. [16], [33] and [34], including steels, aluminum alloys, titanium alloys, and copper. It can be seen in Fig. 4 that the proposed model can describe the trend of ΔK_{thR} v.s. R successfully. Moreover, it is found the data scatter of fatigue crack propagation threshold is much slightly larger than that in Fig. 3 due to the complexity of crack propagation rate test [35].

4. Discussions

4.1. A comparison of the proposed $\Delta\sigma_{eR}$-R model with the existing models

The proposed $\Delta\sigma_{eR}$-R model is further compared with the well-known mean stress correction approaches in terms of simplicity and accuracy. An overview of some existing mean stress correction models as well as their related material constant and fitting parameters is presented in Table 1, where UTS, TTS and YS denote the ultimate tensile strength, true tensile strength and yield strength, respectively; α, γ and k are the related material-dependent parameters. To estimate fatigue properties for a non-zero mean stress, fatigue limit $\Delta\sigma_{e,-1}$ at zero mean stress is indispensable for all the models. Only the Smith-Watson-Topper (SWT) relationship and the

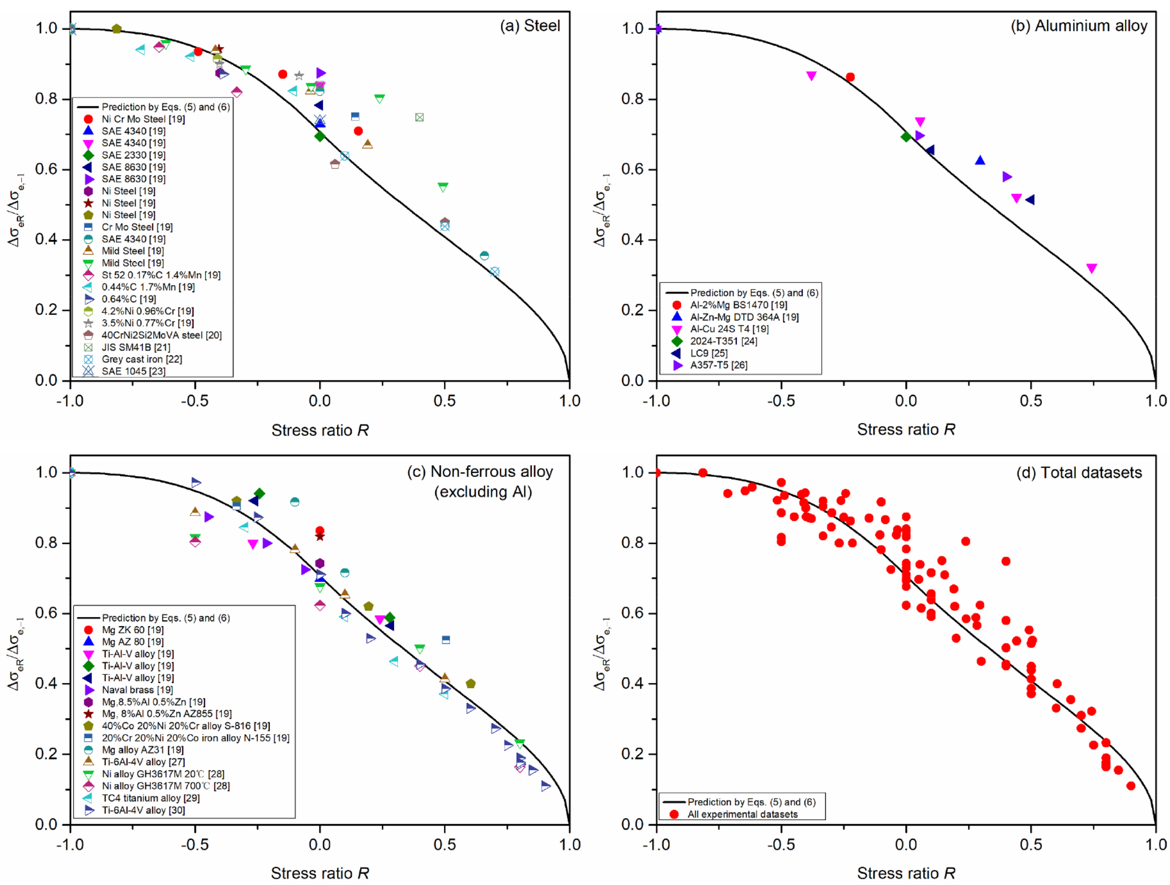

Fig. 3. Validation of the proposed $\Delta\sigma_{eR}$-R model by the experimental datasets taken from literature.

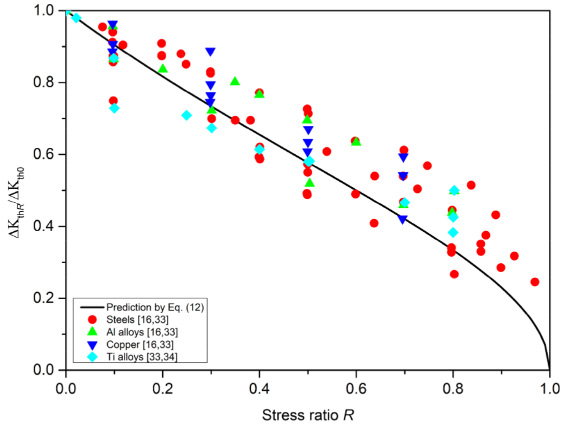

Fig. 4. Validation of the proposed ΔK_{thR}-R model by the experimental datasets in the literature.

Table 1
The existing mean stress correction models.

Model	Equation	Parameters
Smith-Watson-Topper [5]	$\frac{\Delta\sigma_{eR}}{\Delta\sigma_{e,-1}} = \left(\frac{1-R}{2}\right)^{\frac{1}{2}}$	$\Delta\sigma_{e,-1}$
Gerber [4,9]	$\frac{\Delta\sigma_{eR}}{\Delta\sigma_{e,-1}} = \left[1-\left(\frac{\sigma_m}{\mathrm{UTS}}\right)^2\right]$	$\Delta\sigma_{e,-1}$, UTS
Goodman [3]	$\frac{\Delta\sigma_{eR}}{\Delta\sigma_{e,-1}} = 1-\frac{\sigma_m}{\mathrm{UTS}}$	$\Delta\sigma_{e,-1}$, UTS
Smith [36]	$\frac{\Delta\sigma_{eR}}{\Delta\sigma_{e,-1}} = \left(\frac{\mathrm{UTS}-\sigma_m}{\mathrm{UTS}+\sigma_m}\right)$	$\Delta\sigma_{e,-1}$, UTS
Dietmann [37]	$\frac{\Delta\sigma_{eR}}{\Delta\sigma_{e,-1}} = \sqrt{1-\frac{\sigma_m}{\mathrm{UTS}}}$	$\Delta\sigma_{e,-1}$, UTS
Marin [38]	$\frac{\Delta\sigma_{eR}}{\Delta\sigma_{e,-1}} = \sqrt{1-\left(\frac{\sigma_m}{\mathrm{UTS}}\right)^2}$	$\Delta\sigma_{e,-1}$, UTS
Soderberg [39]	$\frac{\Delta\sigma_{eR}}{\Delta\sigma_{e,-1}} = 1-\frac{\sigma_m}{\mathrm{YS}}$	$\Delta\sigma_{e,-1}$, YS
Morrow [40]	$\frac{\Delta\sigma_{eR}}{\Delta\sigma_{e,-1}} = 1-\frac{\sigma_m}{\mathrm{TTS}}$	$\Delta\sigma_{e,-1}$, TTS
Walker [9]	$\frac{\Delta\sigma_{eR}}{\Delta\sigma_{e,-1}} = \left(\frac{1-R}{2}\right)^{\gamma}$	$\Delta\sigma_{e,-1}$, γ
Kwofie [41]	$\frac{\Delta\sigma_{eR}}{\Delta\sigma_{e,-1}} = \exp\left(-\alpha\frac{\sigma_m}{\mathrm{UTS}}\right)$	$\Delta\sigma_{e,-1}$, UTS, α
Sekercioglu [42]	$\frac{\Delta\sigma_{eR}}{\Delta\sigma_{e,-1}} = [1\text{-}\left(\frac{\sigma_m}{\mathrm{YS}}\right)^2\Big]^k$	$\Delta\sigma_{e,-1}$, YS, k

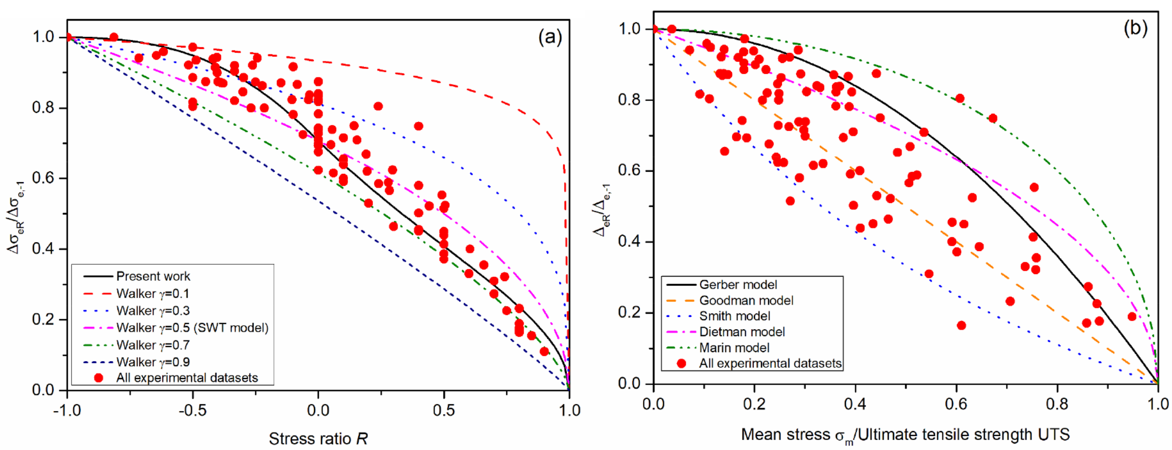

Fig. 5. Comparison of the proposed $\Delta\sigma_{eR}$-R model with other models.

present model have the advantage of being independent of any material constant, while the other correction equations have to introduce the material strength in terms of UTS, TTS or YS, which is easily available. In Walker, Kwofie and Sekercioglu models, a material-dependent fitting parameter is additionally included. Although a reasonable fit over the entire range of the data can be obtained, the physical meaning is ambiguous and the transferability of the fitting parameters is therefore highly questionable. Thus, Kwofie and Sekercioglu models are excluded from the comparison among the existing models and the experimental data in this work. It is worth noting that Walker equation regenerates into SWT if the exponent γ is equal to 0.5.

A direct comparison of the models in a single figure is not straightforward due to the types of the independent variables. Therefore, the accuracy of the models is compared separately based on the independent parameters required by each model. The present work is compared with the SWT model and Walker equation with the assumed exponent γ in terms of normalized fatigue limit-R as shown in Fig. 5a. It can be seen that the proposed model is the most consistent with the experimental results among the models. Fig. 5b shows the comparison of the models in terms of the normalized fatigue limit $\frac{\Delta\sigma_{eR}}{\Delta\sigma_{e,ref}}$ vs. the normalized mean stress $\frac{\Delta\sigma_m}{UTS}$. Comparing Fig. 5b with Fig. 5a, it is found that when the abscissa is expressed in the form of $\frac{\Delta\sigma_m}{UTS}$, the dispersion of the data is much larger than that expressed in the form of R. It is difficult to judge which model is more accurate as shown in Fig. 5b, since most data points fall into the range between the prediction of Smith model and that of Marin model, and Smith model is the most conservative in contrast to the Marin model.

To quantitatively study the accuracy of each model, an analysis of the root mean squared error (RMSE) between the prediction results of each model and the experiment data is carried out. Defining the predicted $\frac{\Delta\sigma_{eR}}{\Delta\sigma_{e,-1}}$ as $\hat{y}_{iR}$ and the experimental $\frac{\Delta\sigma_{eR}}{\Delta\sigma_{e,-1}}$ as y_{iR}, the RMSE can be obtained by:

$$\mathrm{RMSE} = \sqrt{\frac{1}{n}\sum_{i=1}^{n}(\hat{y}_{iR} - y_{iR})^2} \tag{13}$$

where n is the number of the data point. The result is shown in Fig. 6 and it can be clearly seen that the proposed model has the least prediction error compared to the other models. Besides, the prediction accuracy of the Walker model with the γ value of 0.5 (SWT model) is satisfied as well. However, compared with the proposed model, the SWT model overestimates the fatigue limits when $R > 0$ and underestimate the fatigue limits when $R < 0$ (see Fig. 5a).

4.2. A comparison of the proposed ΔK_{thR}-R model with the existing models

Similarly, a comparison of the crack propagation threshold correction model proposed in the present work with the existing model is carried out as well. The used crack propagation threshold correction models are given as follows: [43–45]

$$\frac{\Delta K_{thR}}{\Delta K_{th0}} = 1 - R \quad \text{(Masounaye model [43])} \tag{14}$$

$$\frac{\Delta K_{thR}}{\Delta K_{th0}} = (1 - R)^{1/2} \quad \text{(Davenport model [44])} \tag{15}$$

$$\frac{\Delta K_{thR}}{\Delta K_{th0}} = 1 - R^2 \quad \text{(Grant model [45])} \tag{16}$$

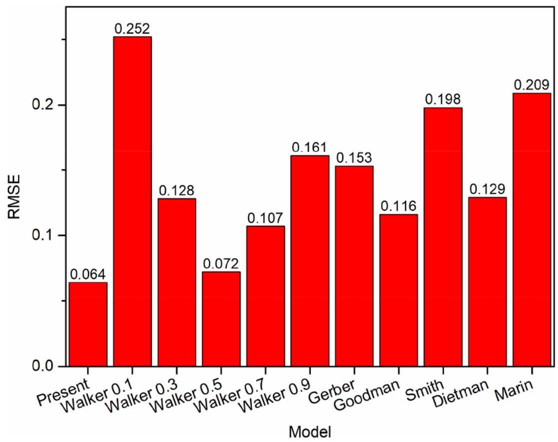

Fig. 6. Error analysis of various fatigue limit correction models.

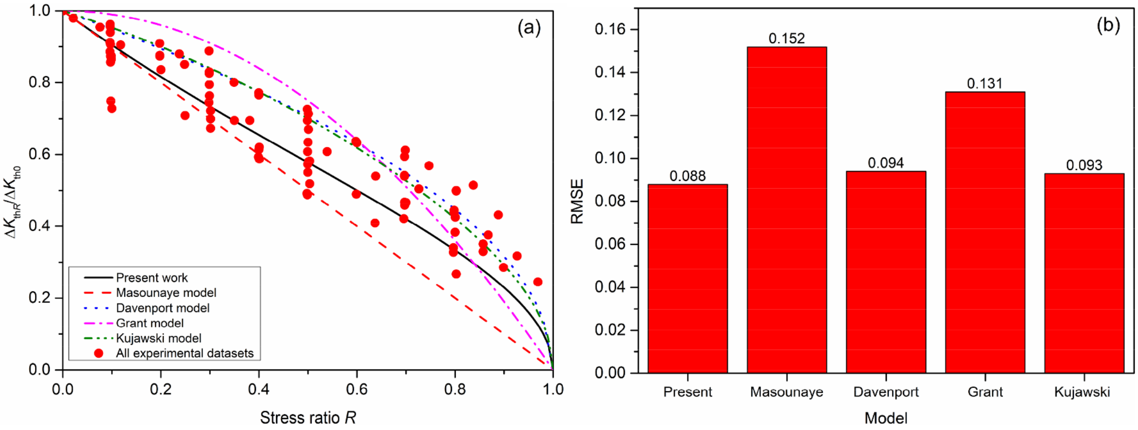

Fig. 7. A comparison of the proposed ΔK_{thR}-R model with the existing models.

$$\frac{\Delta K_{thR}}{\Delta K_{th0}} = \frac{1.8}{\left\{\frac{1+R}{1-R} + \left[\left(\frac{1+R}{1-R}\right)^2 + 4\right]^{1/2}\right\}^{1/2}} \quad \text{(Kujawski model [16])} \tag{17}$$

Fig. 7a shows the comparison of the proposed model and the existing models with experimental data and Fig. 7b displays the corresponding error analysis calibrated by RMSE. Still, the accuracy of the proposed model seems to be the highest.

5. Conclusion

In conclusion, a new mean stress effect correction model of high-cycle fatigue limit is proposed in the work, which is based on the assumption that the needed elastic strain energy leading to fatigue failure is identical under different stress ratios. Based on the proposed mean stress correction of fatigue limit, a unified mean stress correction of fatigue crack propagation threshold is further derived. The proposed models of the two thresholds are verified with various materials, including steels, aluminum alloys and titanium alloys, etc. All the studied materials uniformly collapse into a single normalized $\Delta\sigma_{eR}$-R curve or normalized ΔK_{thR}-R curve. At final, the comparison with the existing models is performed and the accuracy and simplicity of the proposed model is proved.

Declaration of Competing Interest

The authors declare that they have no known competing financial interests or personal relationships that could have appeared to influence the work reported in this paper.

Acknowledgements

The research is financially supported by National Key R&D Program of China (Grant No. 2018YFC0310306) and National Natural Science Foundation of China (NSFC) (Grant No. 51771135).

Appendix A. Supplementary material

Supplementary data to this article can be found online at https://doi.org/10.1016/j.engfracmech.2019.106787.

References

[1] Hou S, Xu J. Relationship among SN curves corresponding to different mean stresses or stress ratios. J Zhejiang Univ-SCIENCE A 2015;16(11):885–93.
[2] Maddox SJ. The effect of mean stress on fatigue crack propagation a literature review. Int J Fract 1975;11(3):389–408.
[3] Goodman J. Mechanics applied to engineering. London: Longmans, Green and Co; 1919.
[4] Gerber H. Bestimmung der zulässigen Spannungen in Eisen-Constructionen. München: Kgl. Hof- u. Universitäts-Buchdruckerei Wolf & Sohn; 1874.
[5] Smith KN, Watson P, Topper TH. A stress-strain function for the fatigue of metals. J Mater 1970;5(4):767–78.
[6] Elber W. The significance of fatigue crack closure. Damage tolerance in aircraft structures. ASTM STP; 1971. p. 230–42.
[7] Zhu ML, Xuan FZ, Tu ST. Effect of load ratio on fatigue crack growth in the near-threshold regime: a literature review, and a combined crack closure and driving force approach. Engng Fract Mech 2015;141:57–77.
[8] Kujawski D. A new (ΔK + Kmax)0.5 driving force parameter for crack growth in aluminum alloys. Int J Fatigue 2001;23(8):733–40.
[9] Walker K. The effect of stress ratio during crack propagation and fatigue for 2024–T3 and 7075–T6 aluminum. ASTM International: Effects of environment and complex load history on fatigue life; 1970.
[10] Kwofie S, Rahbar N. An equivalent driving force model for crack growth prediction under different stress ratios. Int J Fatigue 2011;33(9):1199–204.
[11] Naderi M, Khonsari M. An experimental approach to low-cycle fatigue damage based on thermodynamic entropy. Int J Solids Struct 2010;47(6):875–80.
[12] Yang W, Guo X, Guo Q, Fan J. Rapid evaluation for high-cycle fatigue reliability of metallic materials through quantitative thermography methodology. Int J

Fatigue 2019;124:461–72.
[13] Mehdizadeh M, Khonsari M. On the role of internal friction in low-and high-cycle fatigue. Int J Fatigue 2018;114:159–66.
[14] Guo Q, Guo X, Fan J, Syed R, Wu C. An energy method for rapid evaluation of high-cycle fatigue parameters based on intrinsic dissipation. Int J Fatigue 2015;80:136–44.
[15] Sih GC. Mechanics of Fracture Initiation and Propagation: Surface and Volume Energy Density Applied as Failure Criterion. Dordrecht: Kluwer Academic Publisher; 1991.
[16] Kujawski D. A unified approach to mean stress effect on fatigue threshold conditions. Int J Fatigue 1995;17(2):101–6.
[17] Kitagawa H, Takahashi S. Applicability of fracture mechanics to very small cracks in the early stage. In: Proceedings of the Second International Conference on mechanical behavior of materials ASM; 1976:627–31.
[18] McEvily AJ. Current aspects of fatigue. Metal Sci 1977;11(8–9):274–84.
[19] Forrest PG. Fatigue of metals. Oxford: Pergamon Press; 1962.
[20] Gao Y. Fatigue stress concentration sensitivity and stress ratio effect of a 40CrNi2Si2MoVA steel. Mater Lett 2017;186:235–8.
[21] Tanaka K, Nakai Y. Propagation and non-propagation of short fatigue cracks at a sharp notch. Fatigue Fract Engng Mater Struct 1983;6(4):315–27.
[22] Taylor D. Crack modelling: A technique for the fatigue design of components. Engng Fail Anal 1996;3(2):129–36.
[23] Du Quesnay DL, Yu MT, Topper TH. An Analysis of Notch-Size Effects at the Fatigue Limit. J Test Eval 1988;16(4):375–85.
[24] Zhao SB, Wang ZB. Anti-fatigue design: Methods and Data. Beijing: China Machine Press; 1997. (in Chinese).
[25] Chen ZZ, Xie CH, Zhu CX. Fatigue behaviors of A357 cast aluminum alloy and effects of temperature. Foundry 2010;9(7):700–3. (in Chinese).
[26] Nakai Y, Saka M, Yoshida H, Asayama K, Kikuchi S. Fatigue crack initiation site and propagation paths in high-cycle fatigue of magnesium alloy AZ31. Int J Fatigue 2019;123:248–54.
[27] Liu X, Sun C, Hong Y. Faceted crack initiation characteristics for high-cycle and very-high-cycle fatigue of a titanium alloy under different stress ratios. Int J Fatigue 2016;92:434–41.
[28] Wan AS, Xiong JJ. Effect of stress ratio on HCF and VHCF properties at temperatures of 20 °C and 700 °C for nickel-based wrought superalloy GH3617M. Chin J Aeronaut 2019;32(9):2199–210.
[29] Li W, Zhao H, Nehila A, Zhang Z, Sakai T. Very high cycle fatigue of TC4 titanium alloy under variable stress ratio: Failure mechanism and life prediction. Int J Fatigue 2017;104:342–54.
[30] Morrissey R. Frequency and stress ratio effects in high cycle fatigue of Ti-6Al-4V. Int J Fatigue 1999;21(7):679–85.
[31] Mughrabi H. On 'multi-stage' fatigue life diagrams and the relevant life-controlling mechanisms in ultrahigh-cycle fatigue. Fatigue Fract Engng Mater Struct 2002;25(8–9):755–64.
[32] Murakam Y, Nomoto T, Ueda T. Factors influencing the mechanism of superlong fatigue failure in steels. Fatigue Fract Engng Mater Struct 1999;22(7):581–90.
[33] Kwofie S, Zhu ML. Modeling R-dependence of near-threshold fatigue crack growth by combining crack closure and exponential mean stress model. Int J Fatigue 2019;122:93–105.
[34] Jones R, Michopoulos JG, Iliopoulos AP, et al. Representing crack growth in additively manufactured Ti-6Al-4V. Int J Fatigue 2018;116:610–22.
[35] Zerbst U, Vormwald M, Pippan R, Gänser H-P, Sarrazin-Baudoux C, Madia M. About the fatigue crack propagation threshold of metals as a design criterion – a review. Engng Fract Mech 2016;153:190–243.
[36] Smith JH. Some experiments on fatigue of metals. J Iron Steel Institute 1910;82(2):246–318.
[37] Dietmann H. Festigkeitsberechnung bei mehrachsiger Schwingbeanspruchung. Konstruktion 1973;25(5):181–9.
[38] Marin J. Interpretation of fatigue strengths for combined stresses. Proceedings of International Conference on Fatigue of Metals. 1956. p. 184–95.
[39] Soderberg CR. Factors of safety and working stresses. Trans Am Soc Mech Eng 1939;52:13–28.
[40] Morrow J. Fatigue properties of metals. Section 3.2, Fatigue Design Handbook, Pub. No. AE-4, (Society of Automotive Engineers, Warrendale, PA) 1968:21–29.
[41] Kwofie S. An exponential stress function for predicting fatigue strength and life due to mean stresses. Int J Fatigue 2001;23(9):829–36.
[42] Sekercioglu T. A new approach to the positive mean stress diagram in mechanical design. Materialwiss Werkstofftech 2009;40(9):713–7.
[43] Masounaye J, Bailon JP. The dependence of the threshold stress intensity factor on the cyclic stress ratio in fatigue of ferritic-pearlitic steels. Scr Metall 1975;9(7):723–30.
[44] Davenport RT, Brook R. The threshold stress intensity range in fatigue. Fatigue Fract Engng Mater Struct 1979;1(2):151–8.
[45] Jr Grant, Gallagher J. Fracture toughness and slow stable cracking. ASTM STP 1974;559:225–44.